Hypernetted-chain solutions for the two-dimensional classical electron gas

F. Lado
Department of Physics, North Carolina State University, Raleigh, North Carolina 27607

(Received 2 June 1977)

The hypernetted-chain integral equation is solved numerically to yield the pair correlation function, equation of state, and free energy of a two-dimensional classical electron gas, for values of $\Gamma \equiv (\pi n)^{1/2} e^2/k_B T$ up to 100. The onset of short-range order in the gas is found to occur for $2.8 < \Gamma < 2.9$. In general, the results are qualitatively similar to those of the three-dimensional electron gas.

I. INTRODUCTION

A gas of charged point particles neutralized by a uniform background of opposite charge has long served as the prototypical model of three-dimensional (3D) charged fluids. In the classical regime, the equilibrium properties of this one-component plasma have been studied with Monte Carlo techniques[1,2] and with a variety of approximate approaches. With the Monte Carlo data as the standard, it is found that the best of the approximate results are at present furnished by the hypernetted-chain (HNC) integral equation.[3–6] This equation additionally leads to fulfillment of the Stillinger-Lovett[7] moment conditions on the pair correlation function and reduces properly to the Debye-Hückel form in the limit of a very dilute gas. Thus it seems worthwhile to consider a two-dimensional (2D) version of the HNC equation to study the equilibrium properties of a one-component plasma layer. In this work, we present numerical solutions of the HNC equation for the free energy, internal energy, and pair correlation function of a two-dimensional classical charged gas neutralized by a rigid, uniform background.

This classical model of a two-dimensional (2D) electron gas has received much recent attention,[8–11] stimulated by the laboratory realization[12] of what is in effect such a 2D system: bound electrons in the ground state of a potential well formed above the free surface of liquid helium by an attractive image potential and a repulsive surface barrier, with unconstrained motion parallel to the surface. The electronic area density $n = N/A$ in these experiments is widely variable and under typical conditions the behavior of the trapped electrons may be described classically.[8,9] In this case, the thermodynamic state of the electron gas is determined by the single parameter

$$\Gamma = (e^2/a)/k_B T , \tag{1}$$

giving the ratio of the electrostatic energy at the ion-circle radius a,

$$\pi a^2 n = 1 , \tag{2}$$

to the thermal energy. Here e is to be interpreted as a "renormalized" charge[8,9] incorporating the effects of the dielectric substrate.

For small Γ, the equation of state can be written as an expansion in powers of Γ^2, but the Coulomb potential in two dimensions makes the evaluation of the virial coefficients particularly difficult. The leading correction to the ideal gas equation of state has been determined through summation of ring diagrams by Totsuji[9] and Chalupa[10] to be

$$p/nk_B T - 1 = \Gamma^2(\ln 2\Gamma - \tfrac{1}{2} + \gamma) + \cdots , \tag{3}$$

where $\gamma = 0.5772\ldots$ is Euler's constant. The HNC solutions that will be discussed below agree numerically with this result for $\Gamma \ll 1$. Higher corrections are effectively obtained through the iterative solution of the HNC equation; for large Γ, we find that the reduced pressure depends linearly on Γ.

The long-range nature of the Coulomb potential introduces difficulties for numerical work which become particularly severe in two dimensions, as was also noted above for the virial coefficients. We examine in Sec. II the long-range behavior of the pair correlation function $g(r)$ and related functions. These large-r forms must first be analytically extracted before a numerical solution over a finite range can proceed. A formulation of the problem that accomplishes this is given in Sec. III and the results then obtained from the HNC equation for values of Γ ranging up to $\Gamma = 100$ are discussed in Sec. IV.

II. LONG-RANGE BEHAVIOR

The HNC equation for the pair correlation function g is obtained by supplementing the Ornstein-Zernike equation

$$G(r) \equiv g(r) - 1$$
$$= C(r) + n \int d\vec{r} C(|\vec{r} - \vec{r}|) G(r') \quad , \tag{4a}$$

which defines the direct correlation function C, with the approximate closure[13]

$$C(r) = G(r) - \ln g(r) - \beta v(r) \quad , \tag{4b}$$

where $\beta = (k_B T)^{-1}$ and v is the Coulomb potential here

$$v(r) = e^2/r \quad . \tag{5}$$

The iterative solution of Eqs. (4) can be carried out using Fourier transforms, in terms of which Eq. (4a) becomes

$$\tilde{G}(k) = \tilde{C}(k)/[1 - n\tilde{C}(k)] \quad . \tag{6}$$

We note that in two dimensions the Fourier transform of a circularly symmetric function $F(r)$ becomes a Hankel transform upon integrating over the polar angle:

$$\tilde{F}(k) = \int d\vec{r} F(r) e^{-i\vec{k}\cdot\vec{r}} = 2\pi \int_0^\infty dr\, r F(r) J_0(kr) \quad , \tag{7}$$

with the inverse

$$F(r) = (2\pi)^{-1} \int_0^\infty dk\, k \tilde{F}(k) J_0(kr) \quad . \tag{8}$$

Here $J_0(x)$ is the zeroth-order Bessel function of the first kind.

It is convenient to perform the iterations on the function H, defined by

$$g(r) = \exp[H(r) - \beta v(r)] \quad , \tag{9}$$

rather than on G itself. The coupled Eqs. (4) then become

$$C(r) = G(r) - H(r) = \exp[H(r) - \beta v(r)] - 1 - H(r) \quad , \tag{10a}$$

$$\tilde{H}(k) = n\tilde{C}^2(k)/[1 - n\tilde{C}(k)] \quad . \tag{10b}$$

The numerical evaluation of the transforms in Eqs. (10) must of course be restricted to a finite range in r or k space; if significant error is to be avoided, it is essential that the function being transformed be negligibly small at the termination of this finite range. This will not be the case for the functions C and H, which, as we note below, have long-range Coulomb tails, and thus a necessary step prior to numerical solution will be the analytic extraction of these long-range parts.

It is clear from (4b) or (10a) that the direct correlation function has the usual Coulomb limit for large r,

$$C(r) \sim -\beta v(r) = -\beta e^2/r \quad , \tag{11}$$

so that for small k

$$\tilde{C}(k) \approx -\beta \tilde{v}(k) = -2\pi\beta e^2/k \quad . \tag{12}$$

Using (10b), we have then in the small k limit

$$\tilde{H}(k) \approx 2\pi\beta e^2 k_D/k(k + k_D) \quad , \tag{13}$$

where $k_D = 2\pi\beta e^2 n$ is the Debye wave number. Inversion of Eq. (13) yields the asymptotic form of H:

$$H(r) \sim \beta e^2 k_D \int_0^\infty dk\, J_0(kr)(k + k_D)^{-1} = \beta e^2 k_D \int_0^\infty dt\, e^{-rt} \int_0^\infty ds\, J_0(k_D s) e^{-st}$$
$$= \beta e^2 k_D \int_0^\infty dt\, e^{-rt}(t^2 + k_D^2)^{-1/2} = \tfrac{1}{2}\pi\beta e^2 k_D [\bar{H}_0(k_D r) - Y_0(k_D r)] \quad , \tag{14}$$

where[14] $\bar{H}_0(x)$ and $Y_0(x)$ are the zeroth-order Struve function and Bessel function of the second kind. An expansion of (14) in inverse powers of r can be easily obtained from the last integral in (14), which gives

$$H(r) \sim \frac{\beta e^2}{r} - \frac{\beta e^2 k_D}{(k_D r)^3} + \frac{9\beta e^2 k_D}{(k_D r)^5} - \cdots \tag{15}$$

Our objective now is to remove the asymptotic form (14) from H without, however, introducing infinities at the origin, so that simple subtraction of (14) from H will not do. A suitable long-range function can be produced from (14) and (15) by generalizing to all orders the technique used by Springer, Pokrant, and Stevens[5] in their study of the 3D Coulomb problem. In effect, we weight each r^{-n} term in (15) with a modulating function

$$f_n(r) = 1 - \sum_{j=0}^{n-1} \frac{(\alpha r)^j}{j!} e^{-\alpha r} \quad , \tag{16}$$

where α is a free parameter whose choice is discussed below. Resummation of the new expansion

$$H_l(r) = \frac{\beta e^2}{r} f_1(r) - \frac{\beta e^2 k_D}{(k_D r)^3} f_3(r) + \cdots \tag{17}$$

then yields a function

$$H_l(r) = \beta e^2 k_D \int_0^\alpha dt\, e^{-rt}(t^2 + k_D^2)^{-1/2} \tag{18}$$

which is finite at the origin and has the form (14) for large r; the asymptotic limit is evident upon comparing Eq. (18) with the last integral in (14). The difference function $H - H_l$ will now be properly short-ranged in r space, but, in contrast to the 3D version of this prob-

lem, will at the same time have gained a long-range tail in its transform that $\tilde{H}$ alone did not have. The transform of H_l is readily obtained as

$$\tilde{H}_l(k) = 2\pi\beta e^2 k_D \int_0^\alpha dt\, t(t^2+k_D^2)^{-1/2}(t^2+k^2)^{-3/2} \quad , \tag{19}$$

which for large k gives

$$\tilde{H}_l(k) \sim 2\pi\beta e^2 k_D[(\alpha^2+k_D^2)^{1/2}-k_D]k^{-3}+O(k^{-5}) \quad . \tag{20}$$

The contribution from the leading term in (20) can be non-negligible at the termination of the finite k range, particularly for small Γ. This problem is alleviated by finally choosing for the long-range part of H

$$\begin{aligned} H_L(r) &= H_l(r) - (\beta e^2 k_D/\alpha)[(\alpha^2+k_D^2)^{1/2}-k_D]e^{-\alpha r} \\ &= (\beta e^2 k_D/\alpha)\int_0^\alpha dt\,(\alpha e^{-rt} - te^{-r\alpha}) \\ &\quad \times (t^2+k_D^2)^{-1/2} \quad , \end{aligned} \tag{21}$$

which eliminates the first term in (20), giving a transform $\tilde{H}_L$ of order k^{-5} for large k. This is quite adequate in practice.

Similar considerations dictate the choice

$$\begin{aligned} C_L(r) &= -(\beta e^2/r)(1-e^{-\alpha r}) + \tfrac{1}{2}\beta e^2 \alpha e^{-\alpha r} \\ &= -(\beta e^2/\alpha)\int_0^\alpha dt\,(\alpha e^{-rt} - te^{-r\alpha}) \end{aligned} \tag{22}$$

for the long-range part of C.

It will be noted that Eq. (14), read as an approximate equality for *all* r, is equivalent to the Debye-Hückel approximation. Used with Eq. (9), it yields the nonlinear Debye-Hückel result for g,

$$g(r) \approx e^{-\beta u(r)} \tag{23}$$

$$u(r) = (e^2/r)\{1 - \tfrac{1}{2}\pi k_D r[\bar{H}_0(k_D r) - Y_0(k_D r)]\} \quad , \tag{24}$$

which is valid for low densities. The same approximate H used with (10a), $G = C + H$ and (11) gives the linearized Debye-Hückel g,

$$g(r) \approx 1 - \beta u(r) \quad . \tag{25}$$

In contrast with the three-dimensional case, the linearized form diverges at the origin. Equation (23) was given by Totsuji[9] as an interpolation between the long-range form (25) and the short-range correlation between a single pair of electrons, $\exp(-\beta v)$. Totsuji also notes that Eq. (23) will produce the correct equation of state to order Γ^2 [Eq. (3)].

There will of course be no difference in the g's obtained through Eqs. (9) and (10a) when a self-consistent H is used.

III. FORMULATION FOR NUMERICAL SOLUTION

Define now the short-range functions

$$H_S(r) = H(r) - H_L(r) \quad , \tag{26}$$

$$C_S(r) = C(r) - C_L(r) \quad , \tag{27}$$

where H_L and C_L are given by Eqs. (21) and (22). In terms of these well-behaved functions, the HNC equations become

$$\begin{aligned} C_S(r) &= \exp[H_S(r) + H_L(r) - \beta v(r)] \\ &\quad - H_S(r) - G_L(r) - 1 \quad , \end{aligned} \tag{28a}$$

$$\tilde{H}_S(k) = \frac{\tilde{C}_S(k)+\tilde{C}_L(k)}{1-n[\tilde{C}_S(k)+\tilde{C}_L(k)]} - \tilde{C}_S(k) - \tilde{G}_L(k) \quad , \tag{28b}$$

where

$$G_L(r) \equiv H_L(r) + C_L(r) \quad , \tag{29}$$

and the transforms of H_L and C_L are

$$\begin{aligned} \tilde{H}_L(k) &= 2\pi\beta e^2 k_D \int_0^\alpha dt\,(t^2+k_D^2)^{-1/2} t \\ &\quad \times [(t^2+k^2)^{-3/2} - (\alpha^2+k^2)^{-3/2}] \quad , \end{aligned} \tag{30}$$

$$\begin{aligned} \tilde{C}_L(k) &= -2\pi\beta e^2 k_D \\ &\quad \times \int_0^\alpha dt\, t\,[(t^2+k^2)^{-3/2} - (\alpha^2+k^2)^{-3/2}] \quad . \end{aligned} \tag{31}$$

The integrals over the second term in (30) and both terms in (31) can of course be easily evaluated and we display them in this fashion to bring out similarities. The remaining first term integral in (30) must be numerically evaluated, as must the corresponding integral in (21).

Besides the physical parameter Γ, the numerical parameters to be freely chosen in a calculation are the maximum value R of the radial coordinate, the number of points N in the range $(0,R)$ at which H_S and C_S will be determined, and the "smallness" parameter α, chosen to ensure that $H_S(R)$ and $C_S(R)$ are negligibly small. (A useful rule of thumb has been $\alpha R \approx 20$.) With these parameters given, the numerical Fourier transforms are performed according to the orthogonality-preserving prescription[15]

$$F(r_i) = J_1^2(\mu_i)\sum_{j=1}^{N-1} W_{ij}\hat{F}(k_j) \quad , \tag{32}$$

$$\hat{F}(k_j) = J_1^2(\mu_j)\sum_{i=1}^{N-1} W_{ji}F(r_i) \quad , \tag{33}$$

where

$$\hat{F}(k_j) \equiv \mu_N \tilde{F}(k_j)/2\pi R^2 \quad , \tag{34}$$

$$W_{ij} = W_{ji} = (2/\mu_N)[J_0(\mu_i\mu_j/\mu_N)/J_1^2(\mu_i)J_1^2(\mu_j)] \quad , \tag{35}$$

$$r_i = \mu_i R/\mu_N, \quad i = 1,2,\ldots,N-1 \ , \tag{36}$$

$$k_j = \mu_j/R, \quad j = 1,2,\ldots,N-1 \ , \tag{37}$$

and μ_j is the jth root of $J_0(x)$. The matrix W_{ij} must be computed at the beginning of a calculation and stored, imposing a severe limitation on the size N of the arrays. With W_{ij} defined as a symmetric matrix in (35), the storage needed is reduced from $(N-1)^2$ to essentially half this, at the cost of an extra multiplication in (32) and (33), a worthwhile exchange. It is apparent also that for efficiency transforms should be kept in the form $\mu_N \tilde{F}/2\pi R^2$ during the iterations, with $\tilde{F}$ extracted only at the end. The maximum N in this calculation was $N = 300$.

The iterative solution of Eqs. (28) may be started with $H_S = 0$ and continued until a self-consistent H_S is achieved, this being defined to have occurred whenever the largest difference between the input array H_S into Eq. (28a) and the output H_S from inversion of (28b) is smaller than some preassigned ϵ. In the present calculation $\epsilon = 5 \times 10^{-4}$ was used. For larger values of Γ, H was found to grow roughly linearly with Γ and a considerable number of iterations could be bypassed by using a linear extrapolation of an earlier solution as the initial guess. Other aids for accelerated convergence are discussed by Broyles[16] and Ng.[6]

Finally, the calculation was carried out using dimensionless quantities, specifically a reduced distance $x = r/a$ and a reduced wave number $q = ka$, where a is the ion-circle radius.

IV. RESULTS

The product of the iterative solution of Eqs. (28) is a self-consistent H_S, from which the pair correlation function is obtained as

$$g(r) = \exp[H_S(r) + H_L(r) - \beta v(r)] \ . \tag{38}$$

Figure (1) displays a number of such solutions, ranging from $\Gamma = 1$, for which g still has the monotonic dependence characteristic of the (nonlinear) Debye-Hückel approximation, to $\Gamma = 100$, where g is highly structured. The onset of the oscillations in g occurs for $2.8 < \Gamma < 2.9$. For $\Gamma \ll 1$, the pair correlation function is well described by Eq. (23). Qualitatively, the curves in Fig. (1) are much like the three-dimensional solutions.[5,6] If this parallel holds quantitatively as well, the peaks and valleys in Fig. (1) will be somewhat underestimated compared to Monte Carlo results.

Figures (2) and (3) show the direct correlation function C and structure factor

$$S(k) = 1 + n\tilde{G}(k) \tag{39}$$

for the same values of Γ as in Fig. (1). The similarity with the 3D case is again evident. For all Γ, C differs

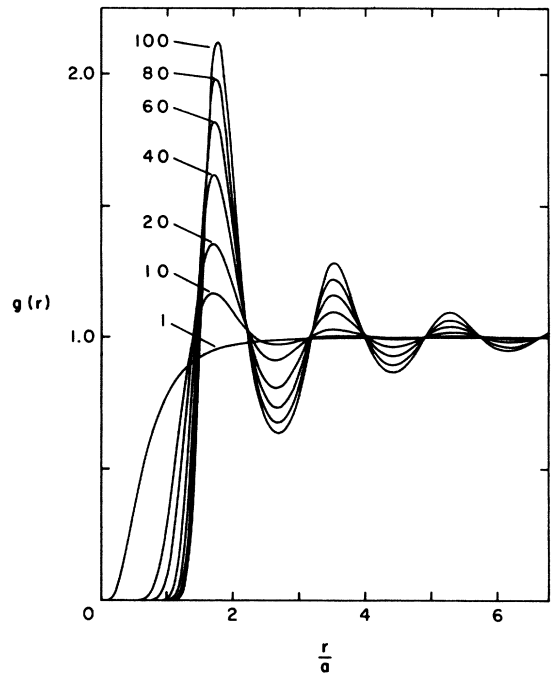

FIG. 1. Pair correlation function of the two-dimensional electron gas for various Γ, as labeled, obtained from the HNC equation.

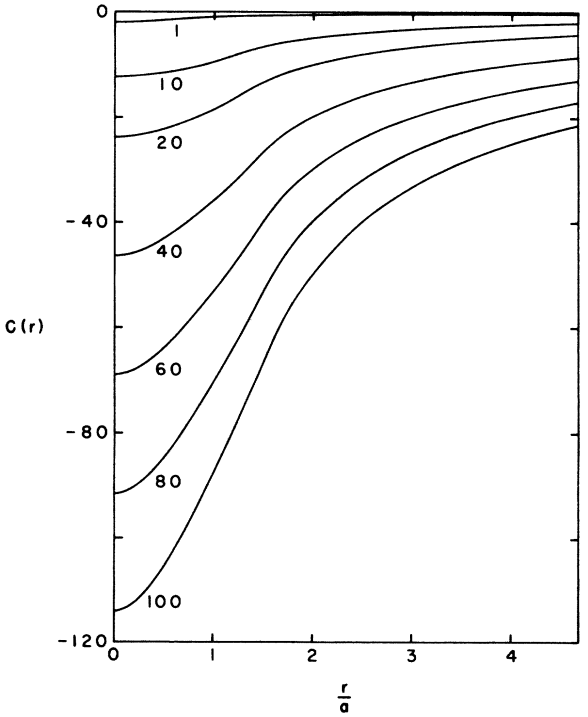

FIG. 2. Direct correlation function of the two-dimensional electron gas for various Γ, as labeled, obtained from the HNC equation.

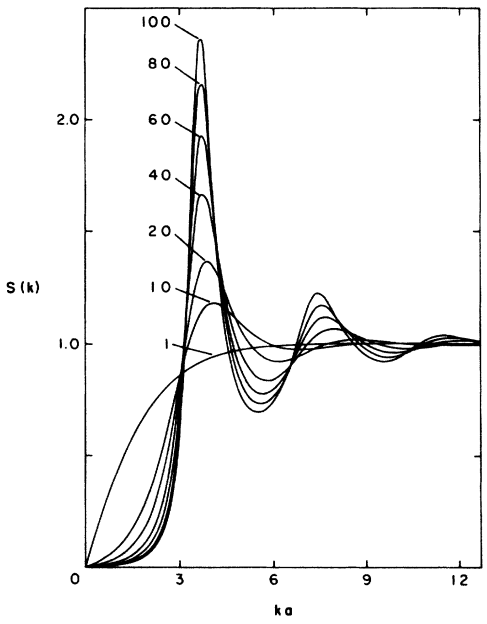

FIG. 3. Structure factor $S(k) = 1 + n\tilde{G}(k)$ of the two-dimensional electron gas for various Γ, as labeled, obtained from the HNC equation.

from the asymptotic limit $-\beta v(r)$ only for relatively short distances, going smoothly to a finite value at the origin. In Fig. (3), we see that S, again for all Γ, vanishes at the origin, reflecting the shielding property of the one-component plasma: the total charge around a given electron is $+e$.

Finally, the thermodynamic properties may be calculated from g. A standard analysis gives the internal energy E and pressure p as

$$\frac{E}{Nk_BT} - 1 = 2\left(\frac{p}{Nk_BT} - 1\right) = \pi n \beta e^2 \int_0^\infty dr G(r) \ . \tag{40}$$

Since for smaller values of Γ, G will decay quite slowly, it is convenient to evaluate this integral in the form

$$\frac{E}{Nk_BT} - 1 = \frac{U_L}{Nk_BT} + \pi n \beta e^2 \int_0^\infty dr\, [G(r) - G_L(r)] \ , \tag{41}$$

where

$$U_L/Nk_BT = \Gamma^2 \{\ln(2k_D/\alpha^2)[(\alpha^2 + k_D^2)^{1/2} - k_D] - \alpha^{-2}[k_D(\alpha^2 + k_D^2)^{1/2} - k_D^2 - \tfrac{1}{2}\alpha^2]\} \tag{42}$$

results from an integration over G_L, defined by Eq. (29), leaving a short-ranged integrand $G - G_L$ in (41) which can be numerically evaluated. The energies obtained from the HNC equation are given in Table I. For $\Gamma \ll 1$, the computed results agree with Eq. (3). As Γ increases, the dependence of the reduced energy on Γ becomes linear and for $\Gamma \gtrsim 30$ can be fitted by

$$E/Nk_BT - 1 = 1.0273 - 1.0967\Gamma \ . \tag{43}$$

TABLE I. HNC values of the excess internal energy and free energy of the classical two-dimensional electron gas.

Γ	$-(E/Nk_BT - 1)$	$-(A - A_0)/Nk_BT$
0.1	0.034	0.024
1	0.781	0.606
5	4.878	4.261
10	10.210	9.273
20	21.026	19.662
30	31.915	30.244
40	42.840	40.920
50	53.786	51.648
60	64.752	62.426
70	75.722	73.218
80	86.687	84.026
90	97.687	94.877
100	108.675	105.729

As noted earlier, the Helmholtz free energy A may be obtained directly from g in the HNC approximation. Adapting the general analysis[17] to the 2D Coulomb gas, we get

$$\frac{A - A_0}{Nk_BT} = (4\pi n)^{-1} \int_0^\infty dk\, k \{n\tilde{G}(k) - \ln[1 + n\tilde{G}(k)]\} - \pi n \int_0^\infty dr\, r[\tfrac{1}{2}G^2(r) + G(r) - g(r)\ln g(r) - G(r)\beta v(r)] \ , \tag{44}$$

where A_0 is the ideal gas free energy. The long-range terms in the second integrand can again be extracted using the functions H_L, C_L, and G_L. The computed results are shown in Table I. For $\Gamma \gtrsim 30$, the reduced free energy is essentially linear in Γ and can be fitted by

$$(A - A_0)/Nk_BT = 0.9851(\ln\Gamma - 0.7540) - 1.0952\Gamma \ . \tag{45}$$

The internal energy resulting from (45), namely,

$$\frac{E}{Nk_BT} - 1 = \Gamma \frac{\partial}{\partial \Gamma}\left(\frac{A - A_0}{Nk_BT}\right) = 0.9851 - 1.0952\Gamma \ , \tag{46}$$

differs only slightly from Eq. (43).

Hockney and Brown[11] have recently studied the properties of the two-dimensional electron gas using a modified molecular dynamics method, wherein the long-range part of the Coulomb $1/r$ potential is incorporated through a coarse-graining technique. Their results differ significantly from those of the HNC equation reported above. We are unable to account for these differences. Earlier work[18] cited by Hockney and Brown for the details of their method does not deal with the $1/r$ potential but rather with the $\ln r$ potential which satisfies the two-dimensional Poisson equation, making a comparison of approximations difficult.

Note added in proof. The results of a Monte Carlo calculation on the $2D$ electron gas have very recently been published by H. Totsuji [Phys. Rev. A 17, 399 (1978)]. The energies obtained from the HNC equation, given in Table I above, agree very well with Totsuji's Monte Carlo values, differing by about 1% or less. Totsuji notes that, within experimental error, his results are consistent with those of Hockney and Brown if the ordinate scale of Fig. 1 in Ref. 111 is shifted to yield the correct Madelung energy at low temperatures.

[1] S. G. Brush, H. L. Sahlin, and E. Teller, J. Chem. Phys. 45, 2102 (1966).

[2] J. P. Hansen, Phys. Rev. A 8, 3096 (1973).

[3] D. D. Carley, J. Chem. Phys. 43, 3489 (1965).

[4] M. S. Cooper, Phys. Rev. A 7, 1 (1973).

[5] J. F. Springer, M. A. Pokrant, and F. A. Stevens, Jr., J. Chem. Phys. 58, 4863 (1973).

[6] K. C. Ng, J. Chem. Phys. 61, 2680 (1974).

[7] F. H. Stillinger and R. Lovett, J. Chem. Phys. 49, 1991 (1968).

[8] A. L. Fetter, Phys. Rev. B 10, 3739 (1974).

[9] H. Totsuji, J. Phys. Soc. Jpn. 39, 253 (1975); 40, 857 (1976).

[10] J. Chalupa, Phys. Rev. B 12, 4 (1975); 13, 2243 (1976).

[11] R. W. Hockney and T. R. Brown, J. Phys. C 8, 1813 (1975).

[12] M. W. Cole, Rev. Mod. Phys. 46, 451 (1974), and references therein.

[13] J. M. J. van Leeuwen, J. Groeneveld, and J. de Boer, Physica (Utr.) 25, 792 (1959); E. Meeron, J. Math. Phys. 1, 192 (1960); T. Morita and K. Hiroike, Prog. Theor. Phys. 23, 1003 (1960); M. S. Green, J. Chem. Phys. 33, 1403 (1960); G. S. Rushbrooke, Physica (Utr.) 26, 259 (1960); L. Verlet, Nuovo Cimento 18, 77 (1960).

[14] *Handbook of Mathematical Functions*, edited by M. Abramowitz and I. A. Stegun (U.S. GPO, Washington, D.C., 1964), p. 496.

[15] F. Lado, J. Comput. Phys. 8, 417 (1971).

[16] A. A. Broyles, J. Chem. Phys. 33, 456 (1960).

[17] T. Morita and K. Hiroike, in Ref. 13; M. S. Green, in Ref. 13.

[18] R. W. Hockney, S. P. Goel, and J. W. Eastwood, Chem. Phys. Lett. 21, 589 (1973); J. Comput. Phys. 14, 148 (1974).